ACS OMEGA

Open Access

http://pubs.acs.org/journal/acsodf

Article

PACS-1 Interacts with TRPC3 and ESyt1 to Mediate Protein Trafficking while Promoting SOCE and Cooperatively Regulating Hormone Secretion

Steven M. Trothen, Jack E. Teplitsky, Ryan E. Armstong, Rong Xuan Zang, Antony Lurie, Mitchell J. Mumby, Cassandra R. Edgar, Matthew W. Grol, and Jimmy D. Dikeakos*

Cite This: *ACS Omega* 2024, 9, 35014−35027

Read Online

ACCESS | Metrics & More | Article Recommendations | Supporting Information

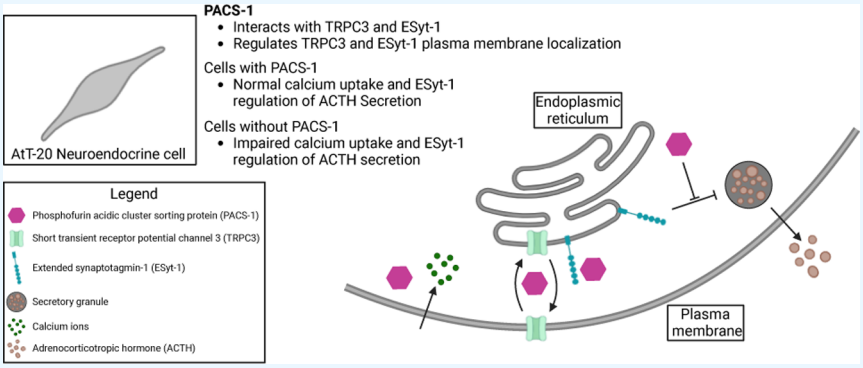

ABSTRACT: Corticotropic cells of the anterior pituitary gland release adrenocorticotropic hormone (ACTH) in a regulated manner to promote the production of cortisol and androgens. The process of ACTH secretion is partly mediated by the phosphofurin acidic cluster sorting protein 1 (PACS-1); however, the underlying mechanisms behind this regulation remain unclear. Herein, we demonstrated PACS-1 interactions with the short transient receptor potential channel 3 (TRPC3) calcium transporter and the extended synaptotagmin-1 (ESyt1) endoplasmic reticulum−plasma membrane tethering protein. Importantly, PACS-1 promoted interactions between TRPC3 and ESyt1 and regulated their plasma membrane localization. Lastly, we demonstrated that PACS-1 is required for a proper store-operated calcium entry (SOCE) response and that ESyt1 regulates ACTH secretion through an unknown mechanism regulated by PACS-1. Overall, our study provides new insights into the physiological role PACS-1 plays in modulating intracellular calcium levels and regulating ACTH secretion in corticotropic cells.

INTRODUCTION

Adrenocorticotropic hormone (ACTH) is an essential peptide hormone that controls the mammalian stress response within the hypothalamus-pituitary-adrenal axis.[1,2] In corticotropic cells within the anterior pituitary gland, pro-opiomelanocortin preproprotein (POMC) is generated and processed into intracellular stores of ACTH, which are secreted following stimulation by secretagogues such as corticotropin releasing factor (CRF) and arginine vasopressin (AVP).[1−3] Following secretagogue stimulation, the plasma membrane (PM) depolarizes, allowing an influx of cytosolic calcium ions (Ca^{2+}) and subsequent activation of protein kinase C (PKC).[4,5] In response to CRH, the primary calcium channels that act to import calcium are voltage-gated calcium channels (VGCCs), allowing Ca^{2+} to enter the cell to stimulate ACTH secretion.[6−9]

Early ACTH secretion can be promoted by releasing intracellular calcium stores from the endoplasmic reticulum (ER) upon lipid hydrolysis of phosphatidylinositol 4,5-biphosphate (PIP_2).[3,9] Specifically, in response to AVP, phospholipase C hydrolyzes PIP_2 into inositol 1,4,5-trisphosphate (IP_3) and diacylglycerol (DAG).[10] Consequently, IP_3 binds to and activates IP_3 receptor (IP3R) calcium channels to induce calcium efflux from the ER.[10] This pathway leads to increased intracellular calcium that promotes ACTH secretion independent of CRF stimulation.[10] In response to CRF, secretion can also be driven by store-operated calcium entry (SOCE).[3] However, pharmacological inhibitors of SOCE can impair initial spikes of ACTH secretion, without affecting

Received: May 27, 2024
Revised: July 19, 2024
Accepted: July 24, 2024
Published: August 3, 2024

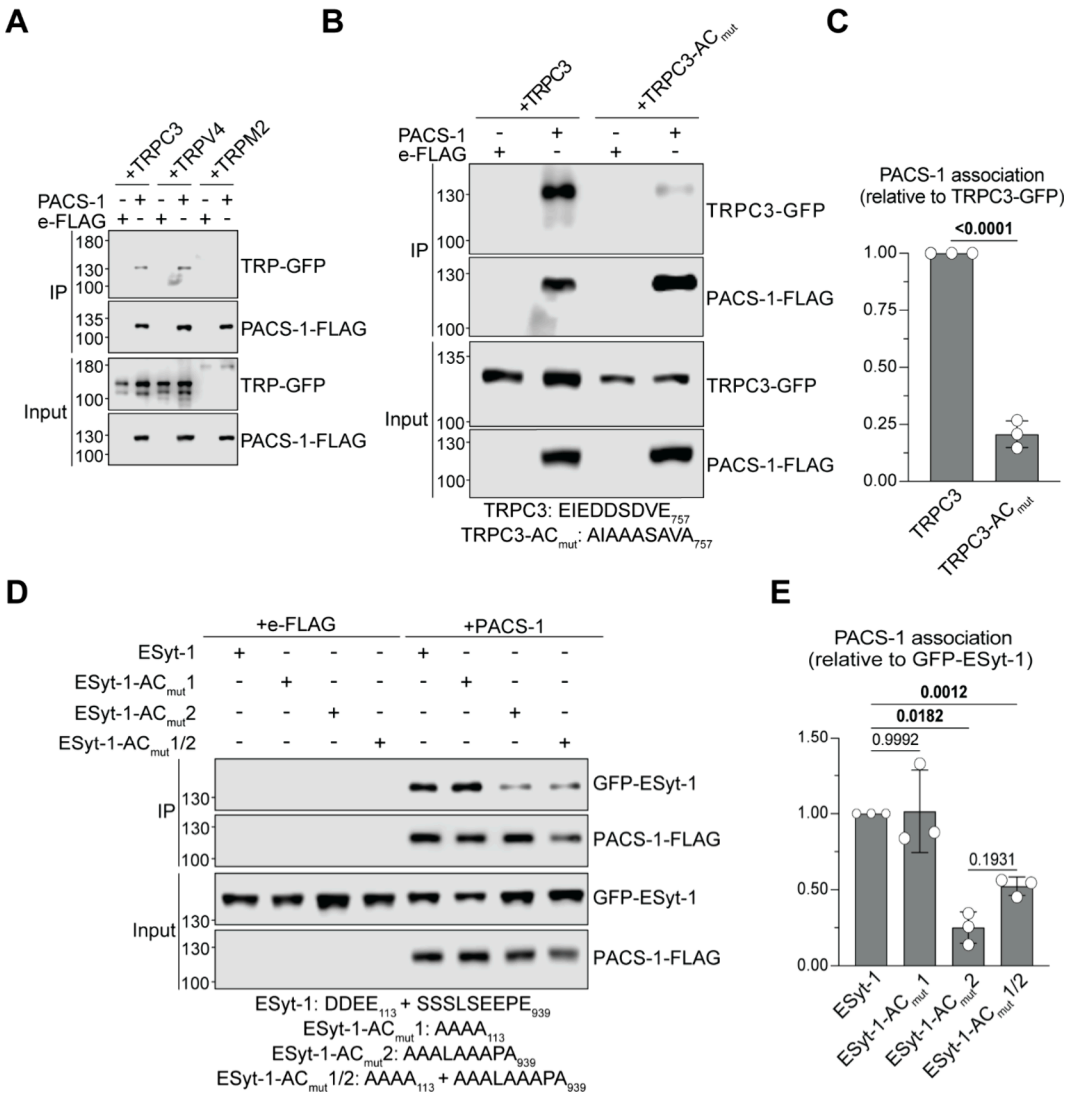

Figure 1. PACS-1 interacts with TRPC3 and ESyt-1 by acidic cluster motifs. A) HEK293T cells were co-transfected with transient receptor short transient receptor potential channel 3, TRPC3-GFP, transient receptor potential melastatin 2, TRPM2-GFP, or vanilloid receptor-related osmotically activated channel osm-9-like TRP channel 4, TRPV4-GFP, and empty-FLAG plasmid e-FLAG, or phosphofurin acidic cluster sorting protein 1, PACS-1-FLAG. Lysates were subjected to co-immunoprecipitation (co-IP) followed by a Western blot (WB) analysis. **B)** HEK293T cells were co-transfected with TRPC3-GFP, TRPC3 acidic cluster mutant TRPC3-AC$_{mut}$-GFP, e-FLAG or PACS-1-FLAG. Lysates were subjected to co-IP and followed by a WB analysis. **C)** Densitometry analysis of TRPC3-AC$_{mut}$-GFP co-IP relative to WT TRPC3-GFP. The amount of TRPC3 pulled down was calculated as [TRPC3-GFP IP/(PACS-1-FLAG IP + TRPC3-GFP input)]; Unpaired students *t* test; 95% confidence interval (α = 0.05); p-value is indicated in the graph; Error bar represents mean ± s.d; N = 3. **D)** HEK293T cells were co-transfected with GFP-ESyt-1, GFP-ESyt-1-AC$_{mut}$1, GFP-ESyt-1-AC$_{mut}$2, GFP-ESyt-1-AC$_{mut}$1/2 and e-FLAG or PACS-1-FLAG. Lysates were subjected to co-IP followed by a WB analysis. **E)** Densitometry analysis of GFP-ESyt-1-AC$_{mut}$ co-IPs relative to WT GFP-ESyt-1. The amount of ESyt-1 pulled down was calculated as [GFP-ESyt-1 IP/(PACS-1-FLAG IP + GFP-ESyt-1 input)]; Nonmatching one-way ANOVA/Tukey's multiple comparisons test; p-values are indicated in the graph; 95% confidence interval (α = 0.05); Error bars represent mean ± s.d; N = 3. All WB images are representative of three independent repeats with approximate molecular weight values in kDa indicated.

the PKC mediated Ca^{2+} influx by L-type VGCCs that mediate sustained stimulated ACTH secretion.[3]

Intracellular calcium levels can be rapidly modulated by low-threshold calcium ion channels, known as transient receptor potential (TRP) cation channels.[11] To import calcium, transient receptor potential canonical (TRPC) channels are activated in response to protein−protein interactions with activated IP3R or lipid−protein interactions between PIP_2 and DAG with lipid-binding sites on TRPCs.[3,12−14] Specifically, the short transient receptor potential channel 3 (TRPC3) is a TRP channel that traffics to the PM and contributes to SOCE by importing calcium into the cytosol and functioning to enhance secretion.[14−18]

Upon calcium store depletion, SOCE channels facilitate Ca^{2+} entry into the cell in parallel with ER calcium influx.[19] SOCE relies on the formation of membrane contact sites (MCSs) between the ER and the PM to import calcium into the cell to replenish ER calcium stores.[19] MCSs can be formed via interactions between calcium-sensitive proteins stromal interaction molecule 1 (STIM1), calcium release-activated calcium channel protein 1 (ORAI1), and extended synaptotagmins, such as extended synaptotagmin-1 (ESyt-1).[19] During SOCE, ESyt1 tethers the ER to the PM and rearranges MCSs

https://doi.org/10.1021/acsomega.4c04998
ACS Omega 2024, 9, 35014−35027

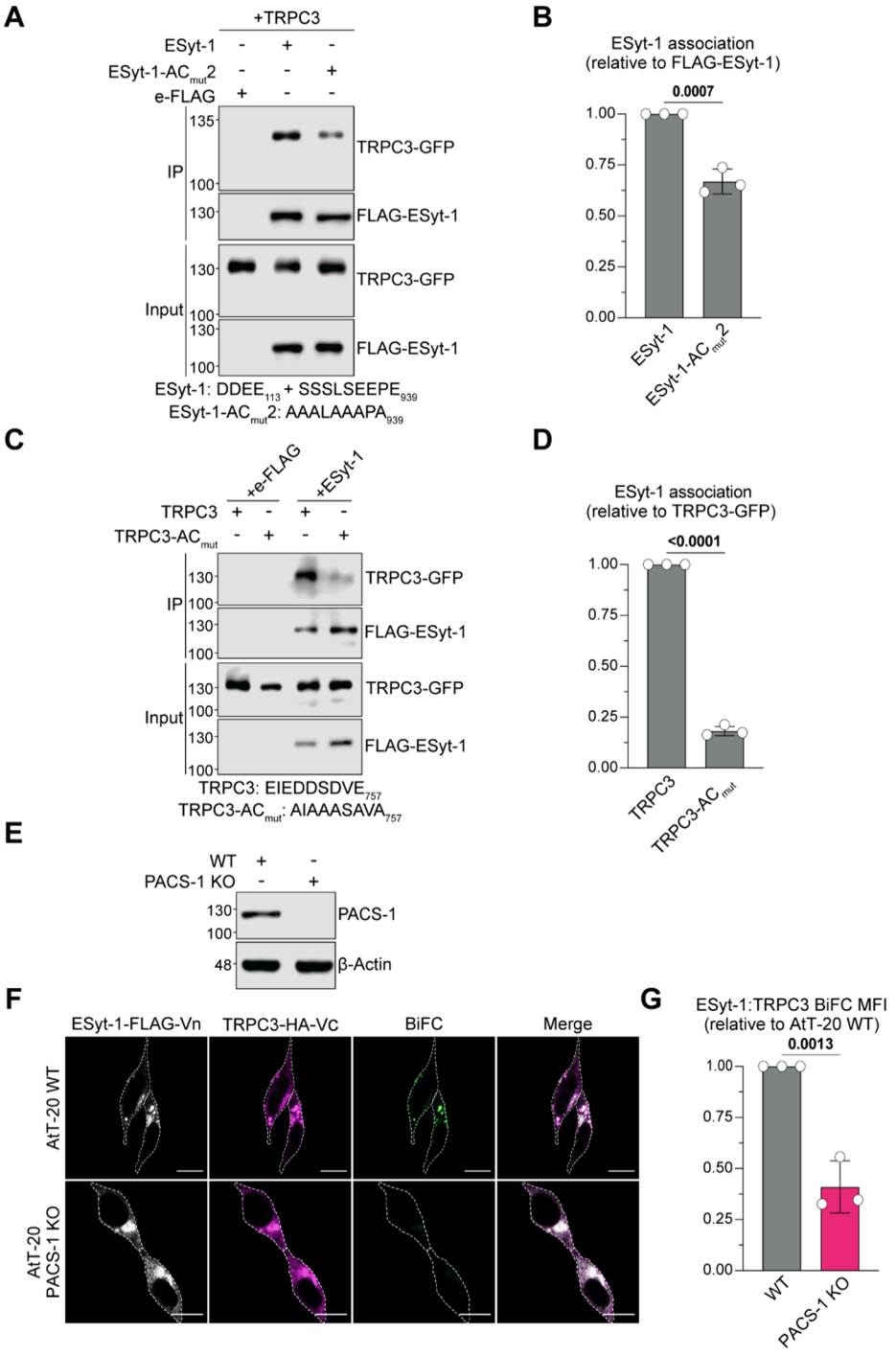

Figure 2. PACS-1 interacting residues promote ESyt-1:TRPC3 interactions. A) HEK293T cells were co-transfected with short transient receptor potential channel 3, TRPC3-GFP, and empty-FLAG plasmid e-FLAG, extended synaptotagmin-1, FLAG-ESyt-1, or ESyt-1 acidic cluster mutant FLAG-ESyt-1-AC$_{mut}$2. Lysates were subjected to co-immunoprecipitation (co-IP) followed by a Western blot (WB) analysis. **B)** Densitometry analysis of TRPC3-GFP co-IP by FLAG-ESyt-1-AC$_{mut}$2 relative to co-IP by FLAG-ESyt-1. The amount of TRPC3 pulled down was calculated as [TRPC3-GFP IP/(FLAG-ESyt-1 IP + TRPC3-GFP input)]. Unpaired students *t* test; p-values are indicated in the graph; 95% confidence interval (α = 0.05); Error bars represent mean ± s.d; N = 3. **C)** HEK293T cells were co-transfected with TRPC3-GFP or TRPC3 acidic cluster mutant TRPC3-AC$_{mut}$-GFP with e-FLAG or FLAG-ESyt-1. Lysates were subjected to co-IP followed by a WB analysis. **D)** Densitometry analysis of TRPC3-AC$_{mut}$-GFP co-IP relative to TRPC3-GFP. The amount of TRPC3 pulled down was calculated as [TRPC3-GFP IP/(FLAG-ESyt-1 IP + TRPC3-GFP input)]; Unpaired students *t* test; p-values are indicated in the graph; 95% confidence interval (α = 0.05); Error bars represent mean ± s.d; N = 3. **E)** WB analysis of whole cell lysates extracted from WT and phosphofurin acidic cluster sorting protein 1 (PACS-1) knockout (KO) AtT-20 cell lines. All WB images are representative of three independent repeats with approximate molecular weight values in kDa indicated. **F)** Representative confocal microscopy images of AtT-20 cells co-transfected with biomolecular fluorescent complementation (BiFC) plasmids ESyt-1-FLAG-Vn and TRPC3-HA-Vc in WT or PACS-1 KO AtT-20 cells. The dashed lines represent the region of interest surrounding the individual AtT-20 cells. The scale bar represents 10 μm, 63× magnification. **G)** ESyt-1-FLAG-Vn:TRPC3-HA-Vc BiFC complex mean fluorescence intensities (MFI) of individual WT (gray) or PACS-1 KO (magenta) AtT-20 cells. Unpaired students *t* test; p-value is indicated in the graph; 95% confidence interval (α = 0.05); Error bar represents mean ± s.d; N = 3, n = 10, 30 cells total.

https://doi.org/10.1021/acsomega.4c04998
ACS Omega 2024, 9, 35014−35027

to accelerate local ER calcium replenishment, where ESyt-1 regulates TRPC3 calcium influx, a key contributor to SOCE.[19,20] Additionally, for TRPC3 to contribute to SOCE, TRPC3 must be dynamically localized to these PIP_2-enriched sites at ER-PM junctions and whether cytosolic trafficking proteins trafficking TRPC3 have a role in this function remains unclear.[16,20,21]

Phosphofurin acidic cluster sorting 1 (PACS-1) is a cytosolic trafficking protein often associated with the trans-Golgi network (TGN) that binds acidic residues termed "acidic clusters" within cargo proteins to regulate their subcellular localization.[22,23] PACS-1 regulates the PM localization and calcium influx activity of TRP channel transient receptor potential cation channel subfamily P member 2 (TRPP2) and previous reports suggest that PACS-1 may interact with additional TRP channels possessing acidic clusters, such as TRPC3.[24] Previous reports also demonstrated that calyculin A promotes the internalization of TRPC3, and brefeldin A redistributes TRPC3 from the Golgi to the ER.[17,25] Importantly, these pharmacological agents inhibit the activity of protein phosphatase 2 and ADP-ribosylation factor 1 (ARF1), respectively, which are key regulators of PACS-1 membrane recruitment and trafficking functions.[22,26] Despite this, potential interaction of PACS-1 with TRPC3 and any subsequent impact on TRPC3 trafficking or calcium homeostasis remain unknown.

Herein, we investigated the role of PACS-1 in calcium homeostasis in corticotropic cells that secrete ACTH. We demonstrated that PACS-1 interacts in a protein−protein complex with TRPC3 and ESyt-1 regulating TRPC3 and ESyt-1 PM localization and trafficking. We have further elucidated interactions between ESyt-1 and TRPC3 and demonstrate the presence of PACS-1 is required for proper SOCE and contributes to ESyt-1 regulation of ACTH secretion. Importantly, these results illustrate how PACS-1 coordinates the PM localization and interaction of calcium-sensitive proteins in ACTH-secreting corticotropic cells.

RESULTS

PACS-1 Interacts with TRPC3 and ESyt-1 at Acidic Cluster Motifs. PACS-1 is known to interact with TRP channels, where PACS-1 regulates the trafficking and function of TRPP2 and forms a protein−protein complex with the vanilloid receptor-related osmotically activated channel osm-9-like TRP channel 4 (TRPV4).[24,27] Thus, we initially assessed if PACS-1 interacts with other TRP channels containing acidic clusters. We did this by performing co-immunoprecipitation (co-IP) analyses of PACS-1 with TRPC3, TRPV4, and the transient receptor potential melastatin 2 (TRPM2). When plasmids were co-expressed in HEK293T cells, PACS-1-FLAG co-immunoprecipitated with TRPC3-GFP but not TRPM2-GFP (Figure 1A). TRPV4 served as a positive control, as PACS-1 and TRPV4 are known to form a protein−protein complex in cells.[24,27] Although we did not detect co-IP of TRPM2-GFP with PACS-1 FLAG, the TRPM2-GFP construct was very lowly expressed, and we can therefore not discount potential interactions between TRPM2 and PACS-1 interactor (Figure 1A).

We next sought to define the TRPC3 motif implicated in the interaction with PACS-1. To conduct its trafficking functions, PACS-1 preferentially binds proteins by interacting with acidic cluster motifs, therefore we tested if the TRPC3 acidic cluster ($EIEDDSVE_{757}$) mediates interactions with PACS-1 via co-IP analyses.[23] Upon co-expression of a TRPC3 acidic cluster mutant, TRPC3-AC_{mut}-GFP ($AIAAASVA_{757}$) and PACS-1-FLAG, there was a dramatic decrease of any PACS-1:TRPC3 complex when normalized to protein expression (Figure 1B,C).

We next investigated putative interactions between PACS-1 and ESyt-1 by co-IP analyses, as ESyt-1 has been shown to regulate TRPC3 current and ESyt-1 also contains two cytosolic acidic clusters ($DDEE_{113}$ and $SSSSLSEEPE_{939}$).[20,28,29] As such, PACS-1-FLAG co-immunoprecipitated GFP-ESyt-1 when both plasmids were co-expressed in HEK293T cells (Figure 1D). We then mutated acidic clusters in ESyt-1, GFP-ESyt-1-AC_{mut}1 ($AAAA_{113}$) and GFP-ESyt-1-AC_{mut}2 ($AAAALAAAA_{939}$) to test for interactions with PACS-1. To test the C-terminal ESyt-1 acidic cluster, we additionally mutated predicted phosphoserines potentially targeted by casein kinase II, which can regulate PACS-1:cargo interactions.[29−31] Intriguingly, the GFP-ESyt-1-AC_{mut}2 ($AAAALAAAA_{939}$) co-IP was reduced when co-expressed with PACS-1-FLAG in HEK293T cells (Figure 1D,E).[29,31] The protein−protein complex was also disrupted when a double acidic cluster mutant, GFP-ESyt-1-AC_{mut}1/2 ($AAAA_{113}$ + $AAAALAAAA_{939}$), was co-expressed with PACS-1-FLAG in HEK293T cells (Figure 1D,E). These results demonstrate that PACS-1 interacts with TRPC3 and ESyt-1 by acidic cluster motifs, and the C-terminal ESyt-1 acidic cluster is necessary for a PACS-1:ESyt-1 protein−protein complex.

PACS-1 Promotes ESyt-1:TRPC3 Interactions. Since we established that PACS-1 interacts with TRPC3 and ESyt-1, we next investigated whether PACS-1 mediates complex formation between ESyt-1 and TRPC3.[20] As such, we tested if ESyt-1 interacted with TRPC3 by co-IP analyses. When plasmids were co-expressed in HEK293T cells, FLAG-ESyt-1 formed a complex with TRPC3-GFP (Figure 2A,C). Intriguingly, the ESyt-1:TRPC3 co-IP was reduced when FLAG-ESyt-1-AC_{mut}2 was co-expressed with TRPC3-GFP, and drastically reduced when FLAG-ESyt-1 was co-expressed with TRPC3-AC_{mut}-GFP in HEK293T cells (Figure 2A−D). Therefore, the acidic clusters that promote PACS-1 interactions with ESyt-1 and TRPC3 also promote interactions between ESyt-1 and TRPC3.

We next investigated if the ESyt-1 and TRPC3 interactions were promoted by PACS-1 within corticotropic cells. To do so, we employed CRISPR/Cas9 to generate a PACS-1 KO AtT-20 cell line where PACS-1 KO was confirmed by the absence of a 130 kDa band corresponding to PACS-1 by WB of whole-cell lysate collected from a clonal AtT-20 population (Figure 2E). To test if PACS-1 mediates interactions between TRPC3 and ESyt-1 in corticotropic cells, we co-expressed BiFC plasmids that produce a fluorescent Venus fluorophore upon close localization and interaction between the Vc and Vn moieties.[32−34] Accordingly, the co-expression of TRPC3-HA-Vc and ESyt-1-FLAG-Vn resulted in a fluorescent protein complex demonstrating a TRPC3:ESyt-1 complex in AtT-20 cells (Figure 2F). Furthermore, compared to WT cells, the TRPC3:ESyt-1 BiFC signal was significantly diminished when TRPC3-HA-Vc and ESYT-1-FLAG-Vn were co-expressed in PACS-1 KO AtT-20 cells (Figure 2F,G). These results suggest that TRPC3:ESyt-1 complex formation is promoted in the presence of PACS-1. Due to the technical challenge of simultaneously expressing three plasmids in AtT-20 cells, we could not confirm the presence of reconstituted PACS-1 in this system.

https://doi.org/10.1021/acsomega.4c04998
ACS Omega 2024, 9, 35014−35027

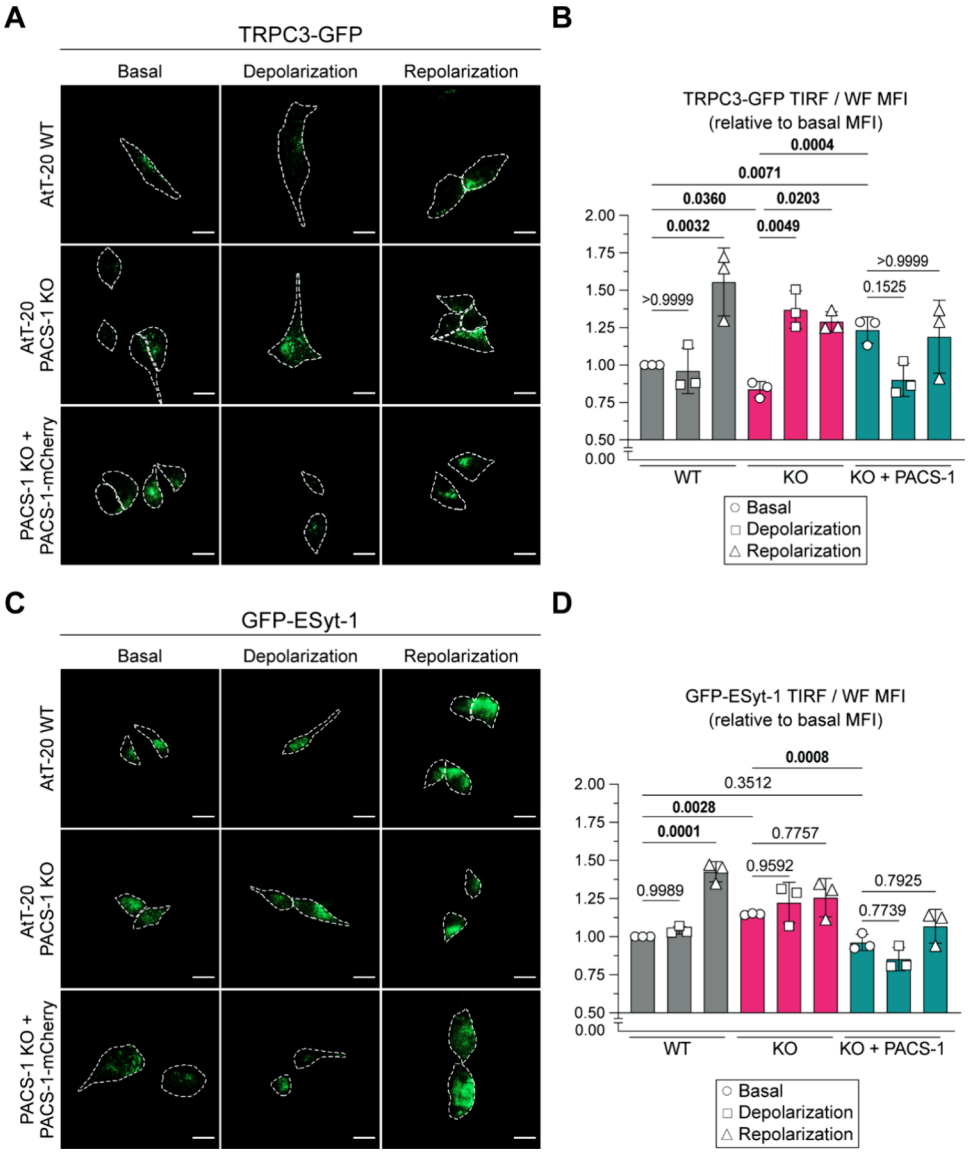

Figure 3. PACS-1 restricts TRPC3 and regulates ESyt-1 plasma membrane localization during depolarization. A, C) Representative total internal reflection fluorescence (TIRF) microscopy images of (A) short transient receptor potential channel 3, TRPC3-GFP, or (C) extended synaptotagmin-1, GFP-ESyt-1, co-transfected with an empty m-Cherry plasmid e-mCherry, or phosphofurin acidic cluster sorting protein 1 (PACS-1)-mCherry, in WT or PACS-1 knockout (KO) AtT-20 cells without treatment (Basal), 10 min after the addition of 80 mM potassium chloride (KCl) (Depolarization), and 10 min after the removal of KCl (Repolarization). The scale bar represents 10 μm, 63× magnification. The dashed lines represent the region of interest surrounding the individual AtT-20 cells in the widefield (WF) channel. **B, D)** TIRF/WF MFI of individual WT (gray), PACS-1 KO (magenta) or PACS-1 KO + PACS-1-mCherry (teal) AtT-20 cells expressing (B) TRPC3-GFP or (D) GFP-ESyt-1 after depolarization (□), or repolarization (△), relative to the basal state (○) of WT AtT-20 cells. Nonmatching one-way ANOVA/Tukey's multiple comparisons test; p-values are indicated in the graph; 95% confidence interval (α = 0.05); Error bars represent mean ± s.d.; N = 3, n = 10, 30 cells total.

PACS-1 Regulates the Plasma Membrane Localization of TRPC3 and ESyt-1. We have established PACS-1, TRPC3 and ESyt-1 as protein interactors; therefore, we next used total internal reflection fluorescence (TIRF) microscopy to observe localization of TRPC3 and ESyt-1 within 110 nm of the PM in the presence or absence of PACS-1. We quantified the TIRF MFI and normalized the TIRF MFI to the MFI in the widefield (WF) channel (TIRF/WF MFI) to account for differences in protein expression across individual cells. Upon quantification, TRPC3-GFP co-expressed with an empty-mCherry plasmid (e-mCherry) showed decreased PM-localization in the PACS-1 KO AtT-20 cells compared to the WT cells (Figure 3A,B). Further, there was a significant increase in TRPC3-GFP TIRF/WF MFI when TRPC3-GFP was co-expressed with PACS-1-mCherry in the PACS-1 KO AtT-20 cells (Figure 3A,B). Conversely, we observed a slight but significant increase in GFP-ESyt-1 TIRF/WF MFI in the PACS-1 KO AtT-20 cells compared to WT cells (Figure 3C,D). Interestingly, GFP-ESyt-1 TIRF/WF MFI was reduced to WT levels when GFP-ESyt-1 was co-expressed with PACS-1-mCherry in PACS-1 KO AtT-20 cells (Figure 3C,D). Therefore, we conclude that PACS-1 promotes the localization of TRPC3 while preventing enhanced ESyt-1 localization at or near the PM.

We hypothesized that the PACS-1 regulation of TRPC3 and ESyt-1 PM localization may affect the pattern of calcium influx

https://doi.org/10.1021/acsomega.4c04998
ACS Omega 2024, 9, 35014−35027

after depolarization. Therefore, we investigated the localization of TRPC3 and ESyt-1 in depolarized cells using TIRF microscopy. Initially, we determined that PACS-1 was trafficked to the PM after depolarization as PACS-1-mCherry TIRF/WF MFI increased following potassium chloride (KCl)-induced depolarization (Figure S1A,B). Furthermore, by removing KCl and allowing cells to repolarize, the PACS-1 TIRF/WF MFI increased further, demonstrating that PACS-1 accumulates at the PM during depolarization and even more so after repolarization (Figure S1A,B).

Examining TRPC3-GFP PM localization in WT and PACS-1 KO AtT-20 cells, we observed that TRPC3-GFP was enriched at the PM in WT cells only after repolarization, where TRPC3 increased its localization at the PM during both depolarization and repolarization in PACS-1 KO cells (Figure 3A,B). ESyt-1 at the PM remained unchanged during depolarization and increased only after repolarization in WT AtT-20 cells (Figure 3C,D). Interestingly, in the PACS-1 KO cells, GFP-ESyt-1 PM localization remained unmodified at the PM during depolarization and repolarization (Figure 3C,D). Correlating widefield images for TIRF TRPC3-GFP and GFP-ESyt-1 TIRF images within Figure 3 are presented (Figure S2A,B). Overall, these observations demonstrate that PACS-1 restricts TRPC3 from the PM during depolarization and promotes ESyt-1 PM localization after depolarization.

We also investigated if PACS-1 regulates the localization of TRPC3 and ESyt-1 within AtT-20 cells using confocal microscopy. TRPC3 localized mainly in the ER and the PM in WT cells, as demonstrated by a moderate colocalization with the diffused ER of AtT-20 cells marked by ER-mCherry, and weak colocalization with the PM marked by wheat germ agglutinin (WGA) (Figure S3A−C). TRPC3-GFP localization with the ER was similar across WT, PACS-1 KO cells, and PACS-1 KO cells expressing exogenous PACS-1-FLAG (Figure S3A,B). WGA colocalization was significantly reduced for TRPC3-GFP in PACS-1 KO cells and returned to WT levels in the presence of PACS-1-FLAG (Figure S3A,C). Interestingly, TRPC3-AC_{mut}-GFP showed reduced PM and increased ER colocalization (Figure S3A−C). The addition of GFP or FLAG tags on PACS-1 or TRPC3 have been previously shown to not affect subcellular localization and interactions with other proteins. Mutation of any acidic cluster within GFP-ESyt-1, and expression of GFP-ESyt-1 or co-expression PACS-1-FLAG in PACS-1 KO AtT-20 cells did not affect ESyt-1 ER or PM localization (Figure S4A−C). Although we did not image FLAG-ESyt-1, the addition of an epitope tag (GFP, Myc, or FLAG) have been demonstrated to mimic the localization of ESyt-1 and maintain its endogenous function.[28,35]

PACS-1 Promotes SOCE and Regulates Calcium Influx Postdepolarization in AtT-20 Cells. Since we demonstrated that TRPC3 and ESyt-1 PM localization were dysregulated in the absence of PACS-1, we then measured the effect of PACS-1 KO on cytosolic calcium levels in AtT-20 cells using live-cell fluorescence microscopy of the cell-permeant ratiometric calcium indicator Fura-2-acetoxymethyl ester (Fura-2-AM). Here we measured changes in intracellular Ca^{2+} using a F340/F380 ratio, representing the ratio of Fura-2-AM emissions captured after excitation at both 340 nm (Ca^{2+} bound state, F340) and 380 nm (Ca^{2+} unbound state, F380). Upon acquiring baseline calcium traces, cells were treated with 2 μM thapsigargin, an inhibitor of the sarcoplasmic/endoplasmic reticulum calcium-ATPases (SERCAs), to deplete ER calcium stores and prime cells for SOCE (Figure 4A).[36] In both WT and PACS-1 KO cell lines, ER calcium efflux occurred almost immediately and peaked within 30 s of exposure to thapsigargin, as indicated by increased F340/F380 ratios above baseline (Figure 4A). The calcium efflux response was higher in WT AtT-20 cells relative to PACS-1 KO cells (Figure 4A). As there was no extracellular Ca^{2+} present, intracellular calcium levels returned to baseline. Next, after 5 min of thapsigargin treatment, we introduced 1 mM of Ca^{2+} to allow for SOCE (Figure 4A). SOCE was heavily impaired in PACS-1 KO cells after Ca^{2+} addition, as the change in peak F340/F380 ratio and total area under the curve (AUC) relative to baseline was decreased compared to WT cells (Figure 4A−C).

As PACS-1 KO cells treated demonstrated impaired SOCE, we also tested if calcium influx following depolarization, a process mainly carried out by L-type voltage-gated channels, was affected.[9] We used Fura-2-AM to monitor KCl-induced depolarization and subsequent Ca^{2+} influx in WT and PACS-1 KO AtT-20 cells (Figure 4D). All cells were capable of prompt Ca^{2+} uptake; however, PACS-1 KO cells demonstrated a steady increase in F340/F380 ratio, whereas a dip in calcium influx was observed in the WT AtT-20 cells (Figure 4D,E). As we observed increased PM-localization of TRPC3 postdepolarization in the PACS-1 KO cells, we hypothesize that increased PM-localized TRPC3 may contribute to sustained calcium influx in depolarized PACS-1 KO cells.

ESyt-1 Works Cooperatively with PACS-1 to Regulate Secretion. AtT-20 cells are a corticotropic neuroendocrine cell line that constitutively produces POMC and secrete ACTH, where PACS-1 is required to sort ACTH and membrane proteins into secretory granules for regulated ACTH secretion.[28,37] Interestingly, ESyt-1 has been previously described as a key regulator of insulin secretion within endocrine cells, and we have established that PACS-1 interacts with ESyt-1, regulating its PM localization within the AtT-20 corticotropic cells.[38] We therefore sought to define if ESyt-1 is implicated in ACTH secretion in coordination with PACS-1.

We first used siRNA against ESyt-1 in WT and PACS-1 KO AtT-20 cells. We observed that knocking down ESyt-1 increased intracellular POMC in WT cells relative to the nontargeting scrambled control (siNS) (Figure 5A). The combined knockdown of ESyt-1 and PACS-1 in AtT-20 WT cells did not increase intracellular POMC compared to the siNS treatment and decreased intracellular POMC compared to the ESyt-1 knockdown (Figure 5A,B). Interestingly, in the PACS-1-KO cell line, there was no difference in intracellular POMC upon ESyt-1 knockdown (Figure 5A,B). ESyt-1 and PACS-1 protein expression for the cell lysates treated with siRNA in Figure 5A was also quantified by densitometry (Figure S5A,B).

Conversely, we tested if overexpression of ESyt-1 and PACS-1 affected intracellular POMC in AtT-20 cells. Accordingly, we observed no effect on intracellular POMC levels when FLAG-ESyt-1 or FLAG-ESyt-1 and PACS-1-HA were expressed in WT AtT-20 cells (Figure 5D,E). Furthermore, we observed increased intracellular POMC when FLAG-ESyt-1 was expressed in PACS-1 KO cells, which was abolished when FLAG-ESyt-1 was co-expressed with PACS-1-HA (Figure 5D,E). This observation suggests ESyt-1 co-operates with PACS-1 to regulate intracellular POMC levels within AtT-20 cells.

We next investigated the supernatant of WT and PACS-1 KO AtT-20 cells to test if ESyt-1 and PACS-1 knockdown also impact ACTH secretion (Figure 5E,F). In line with its effects

https://doi.org/10.1021/acsomega.4c04998
ACS Omega 2024, 9, 35014−35027

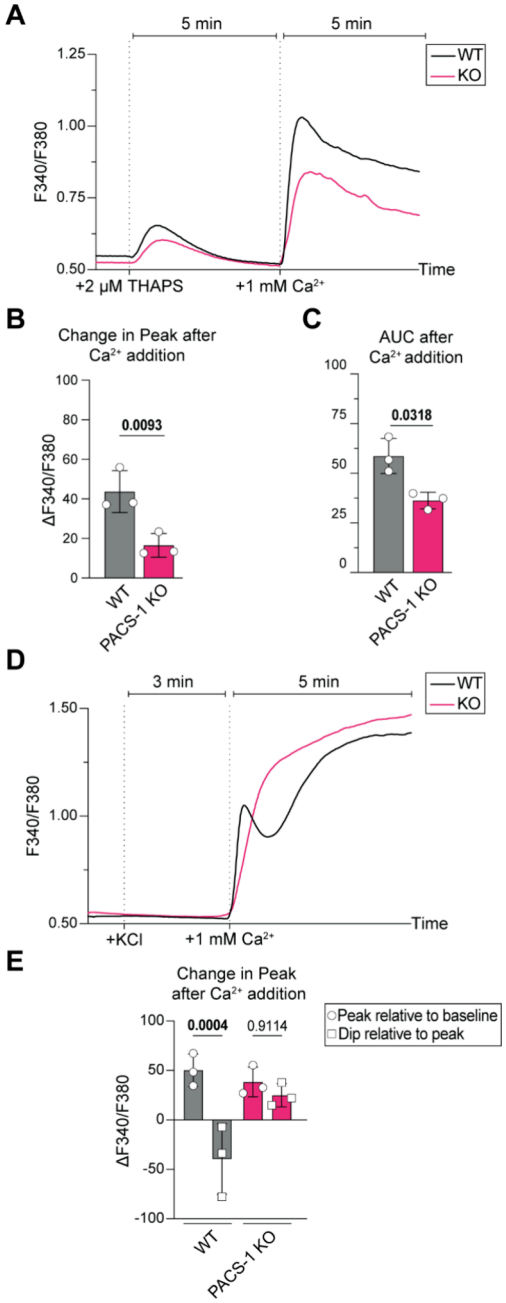

Figure 4. PACS-1 promotes SOCE and regulates calcium influx postdepolarization in AtT-20 cells. A) Fura-2-AM F340/F380 (340 nm excitation/380 nm excitation) ratio in WT and phosphofurin acidic cluster sorting protein 1 (PACS-1) knockout (KO) AtT-20 cells in calcium-free HBSS. Cells were imaged for 2 min to observe the baseline transient Ca^{2+} fluctuations. Cells were then treated with 2 μM thapsigargin (t = 120 s). Five minutes after thapsigargin treatment, dishes were carefully aspirated and HBSS was replaced with an isosmotic HBSS solution containing 1 mM calcium (t = 420 s). N = 3, n = 10, 30 cells total. **B)** Change in maximum F340/F380 value (ΔF340/F380) and **C)** area under the curve (AUC) of F340/F380 ratio after adding 1 mM Ca^{2+} (t = 420 s) relative to average baseline F340/F380 after thapsigargin treatment in WT (gray) and PACS-1 KO (magenta). ΔF340/F380 calculations are described in the methods section. Nonmatching one-way ANOVA/Tukey's multiple comparisons test; p-values are indicated in the graph; Error bars represent mean ± s.d; 95% confidence interval (α = 0.05); N = 3, n = 10, 30 cells total. **D)** Fura-2-AM F340/F380 ratio in WT and PACS-1 KO AtT-20 cells in calcium-free HBSS. Cells were imaged for 2 min. Cells were depolarized with 80 mM potassium chloride (KCl) (t = 120 s). Three minutes after depolarization, exogenous calcium was added to a concentration of 1 mM to allow calcium influx (t = 300 s). N = 3, n = 10, 30 cells total. **E)** ΔF340/F380 of minimum F340/F380 value relative to maximum F340/F380 after Ca^{2+} addition before Ca^{2+} levels rise above initial Ca^{2+} peak in WT (gray) and PACS-1 KO (magenta). Peak F340/F380 relative to average baseline F340/F380 after depolarization and F340/F380 dip relative to peak F340/F380. ΔF340/F380 calculations are described in the methods section. Ordinary two-way ANOVA/Tukey's multiple comparisons test; p-values are indicated in the graph; 95% confidence interval (α = 0.05); Error bars represent mean ± s.d; N = 3, n = 10, 30 cells total.

on intracellular POMC levels, ACTH secretion increased in WT cells when ESyt-1 was knocked down (Figure 5E). Furthermore, the double knockdown of ESyt-1 and PACS-1 in WT cells showed no significant change in ACTH secretion compared to the siNS treatment and decreased ACTH secretion compared to the ESyt-1 knockdown (Figure 5E). Interestingly, ACTH secretion decreased when ESyt-1 was knocked down in PACS-1 KO cells (Figure 5E). Reciprocally, assessing the impact of ACTH secretion by overexpression of FLAG-ESyt-1 alone or with PACS-1-HA had no impact on ACTH secretion in WT cells (Figure 5F). However, ACTH secretion increased when FLAG-ESyt-1 was expressed in PACS-1-KO cells, where this effect was decreased when FLAG-ESyt-1 was co-expressed with PACS-1-HA (Figure 5F). As such, these observations suggest that ESyt-1 negatively regulates ACTH secretion in a manner regulated by PACS-1.

DISCUSSION

PACS-1, along with the related protein PACS-2, are cytosolic trafficking proteins which regulates multiple homeostatic functions.[39,40] In the context of calcium homeostasis, both PACS proteins are essential for TRPP2 function and its shuttling between the ER, Golgi and PM by binding the TRPP2 cytosolic acidic cluster motif $DDSEEDDDEDS_{821}$.[24] Previous reports have also established that PACS-1 can form a protein−protein complex with the TRPV4 calcium channel.[24,27] Herein, we expand the repertoire of acidic cluster calcium channels binding to PACS proteins by identifying PACS-1:TRPC3 interactions within cells (Figure 1).

A previous report demonstrated that truncations of C-terminal cytosolic portions of TRPC3 impacted its ability to import calcium and localize to the PM.[41] These TRPC3 truncations also resulted in mutants that failed to localize at the PM and instead remain sequestered within intracellular compartments.[41] Furthermore, removal of the calmodulin (CaM)/IP3R-binding (CIRB) domain ($TLPPPFSLVPSPKSFV_{790}$) also disrupted TRPC3's PM localization, resulting in its entrapment within intracellular vesicles and the consequent impairment of TRPC3-mediated calcium import.[41] Herein, we demonstrated how TRPC3 removal from the plasma membrane was independent of IP3R/CaM. Instead, PACS-1 engages with TRPC3 through an acidic cluster ($EIEDDSVE_{757}$) upstream of the CIRB site to regulate TRPC3 trafficking (Figures 1B,C and S3).

TRPC3 requires DAG and PIP_2 to localize to ER-PM junctions, and both lipids are modulated by ESyt-1.[38,42] In this regard, we observed that PACS-1 promotes ESyt-1 and TRPC3 interactions in corticotropic cells (Figure 2). We

https://doi.org/10.1021/acsomega.4c04998
ACS Omega 2024, 9, 35014−35027

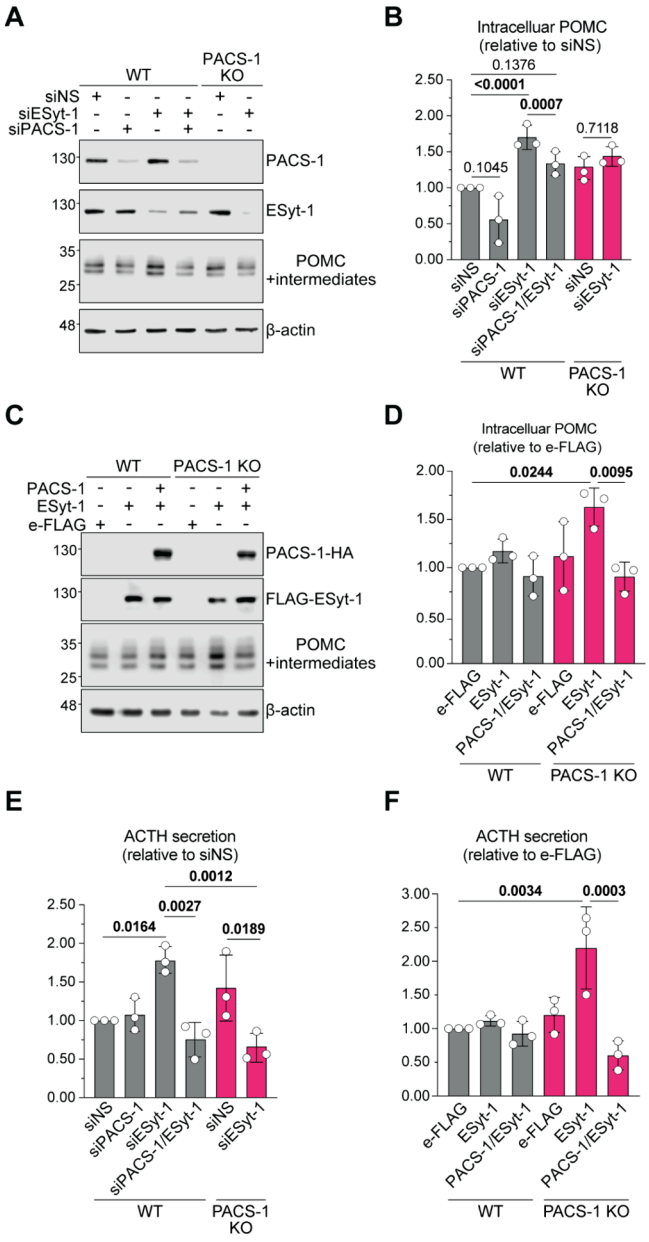

Figure 5. ESyt-1 works cooperatively with PACS-1 to regulate secretion. A) Wildtype (WT) and phosphofurin acidic cluster sorting protein 1 (PACS-1) knockout (KO) AtT-20 cells were transfected with scrambled control nontargeting siRNA (siNS), siRNA targeting PACS-1 (siPACS-1), extended synaptotagmin-1 (ESyt-1) (siESyt-1) or both PACS-1 and ESyt-1 (siPACS-1 + siESyt-1) for 48 h. **B)** Densitometry analysis of WT (gray) and PACS-1 KO (magenta) AtT-20 cells based on the ratio of pro-opiomelanocortin preproprotein (POMC) normalized to ß-actin relative to WT AtT-20 siNS control. Nonmatching one-way ANOVA/Tukey's multiple comparisons test; p-values are indicated in the graph; 95% confidence interval (α = 0.05); Error bars represent mean ± s.d.; N = 3. **C)** WT and PACS-1 KO AtT-20 cells were transfected with empty-FLAG plasmid e-FLAG, FLAG-ESyt-1 or FLAG-ESyt-1 and PACS-1-HA for 48 h. Cell lysates for (A) and (C) were collected and analyzed by Western blot (WB). WB images are representative of three independent repeats with approximate molecular weight values in kDa indicated. **D)** Densitometry analysis of WT (gray) and PACS-1 KO (magenta) AtT-20 cells based on the ratio of POMC and ß-actin relative to WT AtT-20 e-FLAG control. Nonmatching one-way ANOVA/Tukey's multiple comparisons tests; p-values are indicated in the graph; 95% confidence interval (α = 0.05); Error bars represent mean ± s.d.; N = 3. **E)** Secreted adrenocorticotropic hormone (ACTH) in cell supernatant measured by a Luminex MAGPIX assay of WT (gray) and PACS-1 KO (magenta) AtT-20 cells relative to WT AtT-20 siNS control. Nonmatching one-way ANOVA/Tukey's multiple comparisons test; p-values are indicated in the graph; 95% confidence interval (α = 0.05); Error bars represent mean ± s.d; N = 3. **F)** Secreted ACTH in cell supernatant measured by a Luminex MAGPIX assay of WT (gray) and PACS-1 KO (magenta) AtT-20 cells relative to WT AtT-20 e-FLAG control. Nonmatching one-way ANOVA/Tukey's multiple comparisons tests; p-values are indicated in the graph; 95% confidence interval (α = 0.05); Error bars represent mean ± s.d; N = 3.

also observed that the overall ESyt-1 PM-localization was increased while the TRPC3 and ESyt-1 PM-localization were dysregulated during depolarization in the absence of PACS-1 (Figure 3). Therefore, we propose a mechanism where PACS-1 coordinates ESyt-1 and TRPC3 localization to promote their interactions at ER-PM junctions and regulate SOCE. Potentially, PACS-1:TRPC3:ESyt-1 are in a complex in cells where ESyt-1 acts as a calcium sensor to regulate calcium influx by PM-localized TRPC3 or other VGCCs.

The disrupted localization of TRPC3 and ESyt-1, and heavily impaired SOCE, in the absence of PACS-1 highlights a key trafficking function of PACS-1 to maintain calcium homeostasis. Interestingly, we observed that when PACS-1 KO cells are depolarized, calcium entry does not follow the biphasic pattern of the wildtype cell line (Figure 4). This may be a result of increased TRPC3 at the PM in depolarized PACS-1 KO cells; However, ESyt-1 localization is overall increased at the PM but is unaffected by depolarization in the absence of PACS-1 (Figure 3). Thus, we hypothesize that SOCE may be affected by PACS-1 by regulating ESyt-1 and TRPC3 interactions at the ER-PM MCSs, or by affecting other key proteins, such as STIM1 and ORAI1.

We also provide evidence that PACS-1 is critical in mediating ER-calcium efflux, where this effect may result from PACS-1-mediated reduction of IP3R protein expression or modulation of TRPC3 regulation of IP3R (Figure 4).[43,44] Furthermore, PACS proteins are emerging as regulators of mitochondrial structure and apoptosis. Moreover, TRPC3 can regulate mitochondrial calcium uptake and ER calcium release through direct interactions with IP3R.[45−48] Therefore, further investigating if PACS-1 plays a role in maintaining ER-PM MCSs and SOCE, akin to how PACS-2 is involved in regulating ER-mitochondrial contact sites and Ca^{2+} dynamics, may highlight a novel and essential function of PACS-1 in maintaining cellular architecture required for SOCE.[49] However, the mechanism of how PACS-1 mediates intracellular calcium fluctuations is unknown and warrants future investigation.

Lastly, we also demonstrate that ESyt-1 regulates ACTH secretion in AtT-20 corticotropic cells in a manner regulated by the presence of PACS-1. We observed an interesting effect where knocking down ESyt-1 increased intercellular POMC/ACTH secretion in the presence of PACS-1 and overexpressing ESyt-1 increased intercellular POMC/ACTH secretion in the absence of PACS-1. In pancreatic β-cells, ESyt-1 uses a negative feedback loop to regulate insulin secretion, where ESyt-1 regulates DAG microdomain localization to disrupt activated L-type VGCCss at the PM.[38] We

https://doi.org/10.1021/acsomega.4c04998
ACS Omega 2024, 9, 35014−35027

thus speculate that ESyt-1 also contributes to a negative loop in the corticotropic secretion of ACTH, where decreased ESyt-1 levels may reduce DAG transfer, resulting in prolonged periods of ACTH secretion.[38] Contrastingly, increased ESyt-1 expression also augmented intracellular POMC and ACTH secretion in the absence of PACS-1. As these PACS-1 null conditions increased PM-localized ESyt-1, we hypothesize that ESyt-1 fails to localize to DAG PM microdomains, where ESyt-1 would regulate ACTH secretion via lipid exchanges.[38] Interestingly, TRPC3 knockout was recently demonstrated to regulate insulin secretion in murine islet β-cells.[50] Therefore, further elucidating the specific mechanisms PACS-1 uses to regulate the regulated secretory pathways with ESyt-1, and potentially TRPC3, are future avenues for investigation.

CONCLUSIONS

Taken together, we demonstrated that PACS-1 forms protein−protein complexes with the TRPC3 calcium channel and the ESyt-1 ER-PM tethering protein. Furthermore, PACS-1 was essential in promoting TRPC3:ESyt-1 interactions, regulating the PM trafficking of TRPC3 and ESyt-1, and was required for proper SOCE and ACTH secretion in corticotropic cells. Importantly, our results define a key role for PACS-1 in regulating calcium homeostasis, potentially through interactions with TRPC3, and cooperating with ESyt-1 to regulate the secretion of the essential peptide hormone ACTH in corticotropic cells.

METHODS

Cell Culture. Mouse neuroendocrine AtT-20 cells and HEK293T cells (ATCC, Manassas, VA) were passaged with 0.25% trypsin-EDTA (Invitrogen, Waltham, MA) and cultured in complete Dulbecco's modified Eagle's medium (DMEM) (HyClone, Logan, UT) containing 10% fetal bovine serum (Wisent, Montreal, QC) and 100 μg/mL penicillin-streptomycin (HyClone). Cells were grown at 37 °C in 5% CO_2 and subcultured following the suppliers' recommendations. Cultured cells were routinely screened after thawing and throughout passaging for mycoplasma using the MycoAlert mycoplasma Detection Kit (Lonza, Basel, CH).

CRISPR/Cas9-Mediated Knockout of PACS-1. PACS-1 knockout (KO) AtT-20 cells were generated using the following protocol. A total of 2.0 × 10^6 AtT-20 wildtype (WT) cells at an early passage (passage #2 post-thaw) were electroporated with 180 pmol multiguide sgRNAs targeting mouse *PACS1* exon 1 from the Gene Knockout Kit v2 (Synthego, Redwood City, CA) (Guide 1:5′-CGCAGCCGAGGUGGACGAGG-3′/Guide 2:5′-UCGGGCUCUGCGCCUCCGGG-3′/Guide 3:5′-CAUACAAAUUCAUCUGCACU-3′) with 3000 ng Cas9 (Synthego) using the 10 μL Neon electroporation kit (Invitrogen) following suppliers' protocol with the electroporation settings: 1,400 V, 30 ms, pulse number 2. After electroporation, cells were immediately incubated in complete DMEM at 37 °C in 5% CO_2. Twenty-four hours post electroporation, cells were detached with 0.25% trypsin-EDTA (Invitrogen), washed twice with phospho-buffered saline (PBS; Wisent) by centrifugation at 300 × *g*, then incubated with 50 μg/mL propidium iodide (Merck Millipore, Burlington, MA) for 10 min before individual live cell-sorting into 96-well plates using the FACSAria III (13clr 2B-3 V-5YG-3R) cell sorter (London Regional Flow Cytometry Facility, London, ON). Wells with individual cells were expanded into colonies of 30−100 cells before expanding into larger 35 mm wells and T-75 cell culture flasks to screen for PACS-1 protein expression by Western blot (WB) analysis before cryopreservation.

DNA Constructs. PACS-1-mCherry, PACS-1-FLAG (DYKDDDK), and PACS-1-HA (YPYDVPDYA) were previously described.[34,37,44,51] EGFP-ESyt-1 (GFP-ESyt-1) (a gift from Pietro De Camilli, Addgene plasmid # 66830) was used to generate an N-terminal FLAG-tagged FLAG-ESyt-1 using Q5 site-directed mutagenesis (New England Biolabs, Ipswich, MA).[28] Acidic cluster mutants ($AC_{mut}1$, $AC_{mut}2$ and $AC_{mut}1/2$) of GFP-ESyt-1 and FLAG-ESyt-1were generated using Q5 site-directed mutagenesis (New England Biolabs). ESyt-1 was also PCR amplified and cloned into a pcDNA3.1 (Invitrogen) plasmid containing a C-terminal FLAG tag linked to the amino Venus moiety (Vn) to generate ESyt-1-FLAG-Vn. TRPC3-Myc (a gift from Craig Montell Addgene plasmid # 25902) was used to PCR amplify TRPC3 and cloned into a pEGFP-N1 (Clontech, San Francisco, CA) plasmid containing a C-terminal GFP fluorophore to generate TRPC3-GFP. An acidic cluster mutant of TRPC3-GFP (TRPC3-AC_{mut}-GFP) was generated using Q5 site-directed mutagenesis (New England Biolabs). TRPC3-Myc was also used to PCR amplify and cloned into a pcDNA3.1 (Invitrogen) plasmid containing a C-terminal HA tag linked to the carboxy Venus moiety (Vc) to generate TRPC3-HA-VC. TRPM2_pCSdest (a gift from Roger Reeves, Addgene plasmid # 53920) and pcDNA3.0 FLAG TRPV4 (a gift from Robert Lefkowitz, Addgene plasmid # 45751) were used to PCR amplify TRPM2 and TRPV4, respectively, then cloned into a pEGFP-N1 (Clontech) plasmid containing a C-terminal GFP fluorophore to generate TRPM2-GFP and TRPV4-GFP.[52,53] Primers and restriction enzymes used for cloning are available in the Table S1. Sanger sequencing was used to confirm the identity of all DNA constructs (The Centre for Applied Genomics, The Hospital for Sick Children, Toronto, Canada).

Co-immunoprecipitations. A total of 1.5 × 10^6 HEK293T cells were seeded in a 10 cm dish and co-transfected with 2.5 μg of GFP-ESyt-1, GFP-ESyt-AC_{mut}1, GFP-ESyt-1-AC_{mut}2, GFP-ESyt-1-AC_{mut}1/2, TRPC3-GFP, TRPC3-AC_{mut}-GFP with 2.5 μg empty-FLAG (e-FLAG), PACS-1-FLAG, FLAG-ESyt-1, or FLAG-ESyt-1-AC_{mut}2 using 15 μL of PolyJet transfection reagent (SignaGen, Rockville, MS) following the suppliers' protocol. Twenty-four hours post-transfection, cells were washed twice with ice-cold PBS and then incubated in 1× lysis buffer (1.5 mM $MgCl_2$; 1 mM EGTA, 50 mM HEPES, pH 7.4; 150 mM NaCl; 1% Triton X-100; 10% glycerol, supplemented with 1 mM NaF, 2 mM Na_3VO_4 and protease inhibitor cocktail (Roche, Basel, CH)), rocking for 30 min at 4 °C. Cells were then scraped and left rocking for another 30 min at 4 °C. Lysed cells were centrifuged at 21,000 × *g* for 30 min at 4 °C. Cell lysate protein concentrations were determined using the Pierce BCA Protein Assay Kit (Thermo Fisher Scientific, Waltham, MA) and adjusted to 500 μg/mL in 1× lysis buffer for co-IP reactions. Fifty micrograms of protein was resuspended in 5× SDS loading buffer (0.25 M Tris-HCl, pH 6.8; 0.25% bromophenol blue; 10% SDS; 15% ß-mercaptoethanol; 50% glycerol), boiled at 98 °C for 10 min, and stored at −20 °C for use as a 10% input control. Five hundred micrograms of cell lysate was incubated with 2.5 μg of anti-DYKDDDDK antibody (BioLegend, San Diego, CA; 637303) for 15 min, rotating at room temperature (RT). After 15 min, 50 μL of

https://doi.org/10.1021/acsomega.4c04998
ACS Omega 2024, 9, 35014−35027

Protein G Dynabeads (Invitrogen) were added to the cell lysates and incubated for 15 min, rotating at RT. After 15 min, the beads were separated from the cell lysates and washed three times with gentle pipetting of 200 μL PBS containing 0.02% Triton-X. Washed beads were transferred to a clean microcentrifuge tube, resuspended in 50 μL of 1× SDS loading buffer, and boiled at 98 °C for 10 min to elute proteins bound to Protein G Dynabeads. The supernatant was then separated from the beads, transferred to a clean microcentrifuge tube, and stored at −20 °C for WB analysis.

Western Blot Analysis. Ten μL of co-IP reaction, 10% of input control or AtT-20 cell lysate were loaded to each lane of an SDS-polyacrylamide gel. Gels were electroblotted onto Amersham Protran 0.45 μm nitrocellulose membranes (GE Healthcare, Boston, MA) in transfer buffer (25 mM Tris-HCl; 192 mM glycine, pH 8.3; 20% methanol). Nitrocellulose membranes were blocked in tris-buffered saline Tween 20 (TBST) buffer (150 mM NaCl; 10 mM Tris-HCl, pH 8.0; 0.1% Tween 20) with 5% nonfat skim milk powder (BioShop, Burlington, ON) for 40 min before overnight incubation with primary antibodies at 4 °C. Antibodies used are as follows: anti-FLAG (BioLegend, 637303; 1:1000−10,000), anti-GFP (Invitrogen; MA5−15256; 1:2000), anti-PACS-1 (Sigma-Aldrich, St. Louis, MO; HPA 038914; 1:2,000), anti-ESyt-1 (Invitrogen; PA5−53506; 1:2000), anti-POMC/ACTH, an antibody specific to residues 1−18 of ACTH (provided by Dr. Iris Lindberg, University of Maryland; diluted 10 mg/mL; 1:2500), anti-Actin (Invitrogen; MA1−744; 1:5000) and anti-HA (Sigma-Aldrich; H6908; 1:1000). After primary antibody incubation, nitrocellulose membranes were washed three times for 5 min in TBST buffer at RT. Nitrocellulose membranes were incubated with secondary horseradish peroxidase (HRP)-conjugated antibodies for 1 h at RT. Secondary HRP-conjugated antibodies used are as follows: antirat IgG (H+L) (Invitrogen; 31470; 1:2000−1:20,000), antirabbit IgG (H+L) (Invitrogen; 31460; 1:2000−1:5000), and antimouse IgG (H+L) (Invitrogen; 31430; 1:4000−1:10,000). After secondary antibody incubation, nitrocellulose membranes were washed three times for 5 min in TBST buffer at RT and incubated in immobilon Classico or Crescendo chemiluminescent HRP detection reagent (Merck Millipore) for 2 min before imaging with a C−DiGit Blot Scanner (LI-COR Biosciences, Lincoln, NE). Images were collected, and densitometry was performed using IMAGE Studio v5.2 (LI-COR Biosciences).

Bimolecular Fluorescence Complementation. A total of 5.0 × 10^4 WT or PACS-1 KO AtT-20 cells were seeded onto coverslips in a 12-well dish and incubated overnight at 37 °C in the presence of 5% CO_2. The next day, cells were co-transfected with 0.5 μg each of TRPC3-HA-Vc and ESyt-1-FLAG-Vn bimolecular fluorescence complementation (BiFC) plasmids for 48 h using 3.0 μL of P3000 reagent and 7.5 μL of lipofectamine 3000 transfection reagent (Invitrogen) following the suppliers' protocol. Forty-eight hours post-transfection, cells were incubated for 30 min at RT to allow the BiFC signal to mature as previously described.[32,34,55] After fluorophore maturation, coverslips were washed with PBS and fixed in 4% paraformaldehyde (PFA) (Electron Microscopy Sciences, Hatfield, PA) for 15 min at RT, washed three times with PBS, and stained for immunofluorescence (IF) imaging. IF-stained AtT-20 cells were permeabilized with 0.2% Triton X-100 in PBS for 20 min then washed three times with PBS and blocked with Image-IT FX Signal Enhancer (Invitrogen) for 30 min at RT. Blocked cells were washed three times with PBS and incubated in blocking buffer (PBS, 0.1% Triton X-100, 5% bovine serum albumin (Wisent) for 15 min at RT. Next, cells were incubated in a primary antibody for 90 min. Antibodies used are as follows: anti-FLAG (BioLegend; 637303; 1:200) and anti-HA.11 (Biolegend; 991501; 1:200). After primary antibody incubation, cells were washed three times with PBS and incubated with a secondary antibody for 60 min at RT. Secondary antibodies used are as follows: Alexa Fluor 647 AffiniPure Goat Anti-Rat IgG (H+L) (Jackson ImmunoResearch, Philadelphia, PA; 112−605−003; 1:200), and/or Alexa Fluor 594 AffiniPure Goat Anti-Mouse IgG, light chain specific (Jackson ImmunoResearch; 115−858−174; 1:200). After secondary antibody incubation, cells were washed three times in PBS then mounted onto microscope slides in 4′,6-diamidino-2-phenylindole (DAPI) fluoromount (SouthernBiotech, Birmingham, AL) to stain nuclei before confocal microscopy.

Confocal Microscopy. A total of 5.0 × 10^4 WT or PACS-1 KO AtT-20 cells were seeded onto coverslips in a 12-well dish and incubated overnight at 37 °C in the presence of 5% CO_2. The next day, cells were co-transfected with 0.5 μg each of TRPC3-GFP, TRPC3-AC_{mut}-GFP, GFP-ESyt-1, GFP-ESyt-1-AC_{mut}1, GFP-ESyt-1- AC_{mut}2 or GFP-ESyt-1-AC_{mut}1/2 with 0.5 μg ER-mCherry and 0.5 μg e-FLAG or PACS-1-FLAG for 24 h using 3 μL of P3000 reagent and 7.5 μL of lipofectamine 3000 transfection reagent (Invitrogen) following the manufacturer's protocol. Coverslips were stained in 1:1000 dilution of wheat germ agglutinin Alexa Fluor 647 (WGA 647) in prewarmed HBSS for 10 min, washed three times in PBS and fixed in 4% PFA for 15 min at RT, then mounted onto microscope slides in DAPI fluoromount (SouthernBiotech) to stain nuclei. Confocal images were acquired with a Zeiss LSM 880 laser scanning confocal microscope using a Plan-Apochromat 63 × /1.4 NA Oil DIC UVVIS-IR objective (Zeiss, Oberkochen, DE) with 405, 514, 561, and 633 nm laser lines to excite DAPI, Venus, Alexa Fluor 594, and Alexa Fluor 647 fluorophores, respectively, as described previously.[34,54]

Total-Internal-Reflection Fluorescence Microscopy. A total of 5.0 × 10^4 WT and PACS-1 KO AtT-20 cells were seeded in a 35 mm dish with uncoated 14 mm diameter No. 1.5 Coverslips (MatTek, Ashland, MA) and incubated overnight at 37 °C and 5% CO_2. Cells were transfected with 1.0 μg of PACS-1-mCherry alone, 0.5 μg each of GFP-ESyt-1 or TRPC3-GFP and 0.5 μg e-mCherry or 0.5 μg each of GFP-ESyt-1 or TRPC3-GFP and PACS-1-mCherry using 3.0 μL of P3000 and 3.0 μL of lipofectamine 3000 transfection reagent (Invitrogen) following the suppliers protocol. Twenty-four hours post-transfection, cells were washed in prewarmed Hank's balanced salt solution (HBSS; Thermo Fisher Scientific) and fixed in ice-cold methanol for 5 min at −20 °C (Fisher Scientific, Waltham, MA). Fixed cells were washed with HBSS and imaged in 1 mL of HBSS. Images were acquired using a Leica AM TIRF MC microscope TIRF module with an HCX PL APO 63.0 × /1.47 NA oil immersion objective (Leica, Wetzlar, DE) utilizing a 9100−02 EMCCD camera (Hamamatsu, Shizuoka, JP). GFP and DRT filters were used for GFP and mCherry, respectively. TIRF images were collected at 110 nm penetration depth. Raw images were analyzed with ImageJ to calculate mean fluorescence intensities (MFIs).[55]

Intracellular Calcium Imaging. A total of 5.0 × 10^4 of WT or PACS-1 KO AtT-20 cells were seeded in a 35 mm dish with uncoated 14 mm diameter No. 1.5 Coverslips (MatTek)

https://doi.org/10.1021/acsomega.4c04998
ACS Omega 2024, 9, 35014−35027

and incubated overnight at 37 °C and 5% CO_2. Twenty-four hours after seeding, cells were incubated in prewarmed Gibco DMEM (containing high glucose, HEPES, and no phenol red; Thermo Fisher Scientific) with 2 μM Fura-2-AM cell-permeant dye for 30 min at 37 °C and 5% CO_2 (Invitrogen). Before imaging, cells were washed twice with prewarmed Gibco Hank's balanced salt solution without 1 mM calcium (HBSS; Thermo Fisher Scientific; osmolality = 278 ± 5 mOsm/kg H_2O). Calcium imaging was conducted as previously described.[56] Briefly, cells were imaged on a Nikon Eclipse TE2000-U microscope (Nikon, Tokyo, JP) using a Plan Fluor 40 × /0.75 NA oil immersion objective under temperature control at 37 °C in ambient conditions. Cells were excited with alternating 340 and 380 nm wavelengths using a DeltaRam light source (Photon Technology International, PTI, subsidiary of HORIBA, Burlington, ON). Emission filtered (510 ± 20 nm) ratio images were acquired every second with a pco.edge 4.2 LT scientific CMOS camera (PCO-TECH Inc., Romulus, MI) and EasyRatioPro5 Software (PTI).

The calculations used to quantify calcium fluctuations are as follows:

$$\frac{\Delta F340}{F380} = \text{MAX}\,\frac{F340}{F380} - \text{Baseline}\,\frac{F340}{F380}$$

where MAX F340/F380 is the highest observed F340/F380 ratio after t = 420 s and Baseline F340/F380 is the average F340/F380 over t = 389 to t = 419 s.

$$\text{Peak}\,\frac{F340}{F380}\ \text{relative to baseline}\,\frac{F340}{F380} = \frac{\left[\text{MAX}\,\frac{F340}{F380} - \text{Baseline}\,\frac{F340}{F380}\right]}{\text{MAX}\,\frac{F340}{F380}}$$

where MAX F340/F380 is the highest observed F340/F3809 after t = 300 s and baseline F340/F380 is the average F340/F80 between t = 260 s and t = 299 s.

$$\frac{F340}{F380}\ \text{dip relative to peak}\,\frac{F340}{F380} = \frac{\left[\text{MIN}\,\frac{F340}{F380} - \text{MAX}\,\frac{F340}{F380}\right]}{\text{MIN}\,\frac{F340}{F380}}$$

where MAX F340/F380 is the highest observed F340/F3809 after t = 300 s and MIN F340/F380 is the lowest observed F340/F3809 at time after MAX F340/F380.

siRNA Transfections. A total of 2.0 × 10^5 WT or PACS-1 KO AtT-20 cells were seeded in a 35 mm 6-well dish and incubated overnight at 37 °C in 5% CO_2. The next day, cells were transfected with 3.0 μL of 10 μM Silencer select negative control No. 1 siRNA (Invitrogen; 4390843), 10 μM Silencer select anti-PACS-1 siRNA (Invitrogen; s99032), 10 μM Silencer select anti-ESyt-1 siRNA (Invitrogen; s76666), or 1.5 μL of both 10 μM Silencer select anti-PACS-1 siRNA and anti-ESyt-1 siRNA Silencer with 9.0 μL of Lipofectamine RNAiMax (Invitrogen) following the suppliers' protocol. Cells were then incubated at 37 °C for 48 h in the presence of 5% CO_2 before measuring intracellular POMC by WB or measuring ACTH secretion by MAGPIX (Luminex Corporation, Austin, TX). AtT-20 cell lysates were adjusted to 1000 μg/mL with 1× lysis buffer using the Pierce BCA Protein Assay Kit (Thermo Fisher Scientific).

Plasmid Transfections. A total of 2.0 × 10^5 WT or PACS-1 KO AtT-20 cells were seeded in a 35 mm 6-well dish and incubated overnight at 37 °C in 5% CO_2. The next day, cells were transfected with 5.0 μg of e-FLAG, or 2.5 μg each of e-FLAG and FLAG-ESyt-1, or FLAG-ESyt-1 and PACS-1-HA for 48 h using 15 μL of P3000 reagent and 15 μL of lipofectamine 3000 transfection reagent (Invitrogen) following the suppliers' protocol. Cells were then incubated for 48 h at 37 °C in 5% CO_2 before measuring intracellular POMC by WB or ACTH secretion by MAGPIX (Luminex Corporation). AtT-20 cell lysates were adjusted to 1000 μg/mL with 1× lysis buffer using the Pierce BCA Protein Assay Kit (Thermo Fisher Scientific).

Hormone Secretion Assays. AtT-20 cells transfected with siRNA or plasmid DNA were washed twice with prewarmed PBS (Wisent) and incubated in 1 mL of fresh complete DMEM (Wisent) for 2 h at 37 °C in 5% CO_2. Subsequently, cell supernatants were collected and centrifuged at 10,000 × g for 10 min at 4 °C for clarification, transferred to a clean microcentrifuge tube, and stored at −80 °C. Cellular supernatants were subjected to MAGPIX (Luminex Corporation) analysis using the ACTH MILLIPLEX MAP mouse pituitary magnetic bead panel (Merck Millipore) following the suppliers' protocols.

Statistical Analysis and Software. Statistical analysis was performed with GraphPad Prism v9.5.1 software (GraphPad Software). The Shapiro-Wilk test was performed to assess whether the data were parametric or nonparametric, and the proper statistical tests were applied as specified in the figure legends.[57]

■ ASSOCIATED CONTENT

Data Availability Statement

The data supporting the findings of this study are available within the article and its Supporting Information. In addition, the supporting data are available upon reasonable request from the corresponding author (jimmy.dikeakos@uwo.ca).

Supporting Information

The Supporting Information is available free of charge at https://pubs.acs.org/doi/10.1021/acsomega.4c04998.

Additional information containing experimental results, correlating wide-field images, densitometry quantifications, and primers/restriction enzymes used in DNA cloning (PDF)

■ AUTHOR INFORMATION

Corresponding Author

Jimmy D. Dikeakos − *Department of Microbiology and Immunology, Schulich School of Medicine and Dentistry, The University of Western Ontario, London, ON N6A 5C1, Canada;* orcid.org/0000-0001-8141-5395; Email: jimmy.dikeakos@uwo.ca

Authors

Steven M. Trothen − *Department of Microbiology and Immunology, Schulich School of Medicine and Dentistry, The University of Western Ontario, London, ON N6A 5C1, Canada*

Jack E. Teplitsky − *Department of Microbiology and Immunology, Schulich School of Medicine and Dentistry, The University of Western Ontario, London, ON N6A 5C1, Canada*

Ryan E. Armstong − *Department of Physiology and Pharmacology, Schulich School of Medicine and Dentistry, The University of Western Ontario, London, ON N6A 5C1, Canada*

Rong Xuan Zang − *Department of Microbiology and Immunology, Schulich School of Medicine and Dentistry, The*

https://doi.org/10.1021/acsomega.4c04998
ACS Omega 2024, 9, 35014−35027

University of Western Ontario, London, ON N6A 5C1, Canada

Antony Lurie − *Department of Microbiology and Immunology, Schulich School of Medicine and Dentistry, The University of Western Ontario, London, ON N6A 5C1, Canada*

Mitchell J. Mumby − *Department of Microbiology and Immunology, Schulich School of Medicine and Dentistry, The University of Western Ontario, London, ON N6A 5C1, Canada*

Cassandra R. Edgar − *Department of Microbiology and Immunology, Schulich School of Medicine and Dentistry, The University of Western Ontario, London, ON N6A 5C1, Canada;* orcid.org/0009-0009-2392-7670

Matthew W. Grol − *Department of Physiology and Pharmacology, Schulich School of Medicine and Dentistry, The University of Western Ontario, London, ON N6A 5C1, Canada*

Complete contact information is available at: https://pubs.acs.org/10.1021/acsomega.4c04998

Author Contributions

S.M.T. and J.D.D. conceptualization; S.M.T. validation; S.M.T. formal analysis; S.M.T., M.W.G., and J.D.D investigation; M.W.G. and J.D.D. resources; S.M.T. data curation; S.M.T. and J.D.D. writing—original draft; S.M.T. visualization; S.M.T., J.E.T., R.E.A., R.X.Z., A.L., M.J.M., C.R.E., M.W.G., and J.D.D. writing—review and editing; J.D.D. supervision; J.D.D. funding acquisition.

Notes

The authors declare no competing financial interest.

■ ACKNOWLEDGMENTS

This work was supported by a Discovery Grant to J.D.D. from the Natural Sciences and Engineering Council of Canada (NSERC to J.D.D. #04094). M.W.G. was supported by funding from the Canada Research Chairs Program, the Canadian Institutes of Health Research, and NSERC. R.E.A. was a recipient of a Summer Undergraduate Studentship Award from the Bone and Joint Institute at the University of Western Ontario. S.M.T. is a recipient of an RGE Murray Scholarship from the University of Western Ontario. M.J.M. and C.R.E. are recipients of Ontario Graduate Scholarships from the Ontario Government. RX.Z., A.L. and J.E.T. were recipients of Canada Graduate Scholarships—Master's program from the Canadian government. We thank Kristin Chadwick for performing flow cytometry and cell sorting to generate the PACS-1 KO AtT-20 cell line and Dr. Bryan Heit for providing the wheat germ agglutinin Alexa Fluor 647 and ER-mCherry plasmid.

■ ABBREVIATIONS

AC, acidic cluster; AC_{mut}, acidic cluster mutant; ACTH, adrenocorticotropic hormone; ARF1, ADP-ribosylation factor 1; AUC, area under the curve; AVP, arginine vasopressin; BiFC, bimolecular fluorescence complementation; co-IP, co-immunoprecipitation; CRF, corticotropin-releasing factor; DAG, diacylglycerol; DAPI, 4′,6-diamidino-2-phenylindole; DMEM, Dulbecco's modified Eagle's medium; ER, endoplasmic reticulum; ESyt-1, extended synaptotagmin-1; Fura-2-AM, fura-2-acetoxymethyl ester; HBSS, Hank's balanced salt solution; HRP, horseradish peroxidase; IF, immunofluorescence; IP_3, inositol 1,4,5-trisphosphate; IP3R, IP_3 receptor; KCl, potassium chloride; KO, knockout; MCS, membrane contact site; ORAI1, calcium release-activated calcium channel protein 1; PACS-1, phosphofurin acidic cluster sorting protein 1; PFA, paraformaldehyde; PIP_2, phosphatidylinositol 4,5-biphosphate; PM, plasma membrane; POMC, pro-opiomelanocortin preprotein; RT, room temperature; SERCA, sarcoplasmic/endoplasmic reticulum calcium-ATPase; SOCE, store-operated calcium entry; STIM1, stromal interaction molecule 1; TBST, Tris-buffered saline Tween 20; TGN, trans-Golgi network; TIRF, total-internal-reflection fluorescence; TRP, transient receptor potential; TRPC3, short transient receptor potential channel 3; TRPM2, transient receptor potential melastatin 2; TRPP2, transient receptor potential cation channel subfamily P member 2; TRPV4, vanilloid receptor-related osmotically activated channel osm-9-like TRP channel 4; Vc, carboxy Venus; Vn, amino Venus; WB, Western blot; WGA, wheat germ agglutinin

■ REFERENCES

(1) Childs, G. V.; Marchetti, C.; Brown, A. M. Involvement of Sodium Channels and Two Types of Calcium Channels in the Regulation of Adrenocorticotropin Release. *Endocrinology* **1987**, *120*, 2059−2069.

(2) Loechner, K. J.; Kream, R. M.; Dunlap, K. Calcium currents in a pituitary cell line (AtT-20): differential roles in stimulus-secretion coupling. *Endocrinology* **1996**, *137*, 1429−1437.

(3) Yamashita, M.; Oki, Y.; Iino, K.; Hayashi, C.; Yogo, K.; Matsushita, F.; Sasaki, S.; Nakamura, H. The role of store-operated Ca2+ channels in adrenocorticotropin release by rat pituitary cells. *Regul. Pept.* **2009**, *156*, 57−64.

(4) Deng, Q.; Riquelme, D.; Trinh, L.; Low, M. J.; Tomić, M.; Stojilkovic, S.; Aguilera, G. Rapid Glucocorticoid Feedback Inhibition of ACTH Secretion Involves Ligand-Dependent Membrane Association of Glucocorticoid Receptors. *Endocrinology* **2015**, *156*, 3215−3227.

(5) Gambacciani, M.; Liu, J. H.; Swartz, W. H.; Tueros, V. S.; Rasmussen, D. D.; Yen, S. S. C. Intrinsic Pulsatility of ACTH Release from the Human Pituitary *In Vitro*. *Clin. Endocrinol.* **1987**, *26*, 557−563.

(6) Armstrong, C. M.; Hille, B. Voltage-Gated Ion Channels and Electrical Excitability. *Neuron* **1998**, *20*, 371−380.

(7) Catterall, W. A. Structure and Function of Voltage-Gated Ion Channels. *Annu. Rev. Biochem.* **1995**, *64*, 493−531.

(8) Bezanilla, F. Voltage-Gated Ion Channels. *IEEE Trans. Nanobiosci.* **2005**, *4*, 34−48.

(9) Stojilković, S. S.; Izumi, S.; Catt, K. J. Participation of voltage-sensitive calcium channels in pituitary hormone release. *J. Biol. Chem.* **1988**, *263*, 13054−13061.

(10) Lee, A. K.; Tse, F. W.; Tse, A. Arginine Vasopressin Potentiates the Stimulatory Action of CRH on Pituitary Corticotropes via a Protein Kinase C−Dependent Reduction of the Background TREK-1 Current. *Endocrinology* **2015**, *156*, 3661−3672.

(11) Clapham, D. E.; Runnels, L. W.; Strübing, C. The trp ion channel family. *Nat. Rev. Neurosci.* **2001**, *2*, 387−396.

(12) Zhu, M. X.; Tang, J. TRPC Channel Interactions with Calmodulin and IP3 Receptors. In *Novartis Foundation Symposia*; Chadwick, D. J., Goode, J., Eds.; John Wiley & Sons: Chichester, U.K., 2008; pp 44−62. DOI: 10.1002/0470862580.ch4.

(13) Erkan-Candag, H.; Clarke, A.; Tiapko, O.; Gsell, M. A.; Stockner, T.; Groschner, K. Diacylglycerols interact with the L2 lipidation site in TRPC3 to induce a sensitized channel state. *EMBO Rep.* **2022**, *23*, No. e54276.

(14) Kim, M. S.; Lee, K. P.; Yang, D.; Shin, D. M.; Abramowitz, J.; Kiyonaka, S.; Birnbaumer, L.; Mori, Y.; Muallem, S. Genetic and Pharmacologic Inhibition of the Ca2+ Influx Channel TRPC3 Protects Secretory Epithelia From Ca^{2+}-Dependent Toxicity. *Gastroenterology* **2011**, *140*, 2107−2115.

(15) Li, H.-S.; Xu, X.-Z. S.; Montell, C. Activation of a TRPC3-dependent cation current through the neurotrophin BDNF. *Neuron* **1999**, *24*, 261−273.
(16) Hartmann, J.; Dragicevic, E.; Adelsberger, H.; Henning, H. A.; Sumser, M.; Abramowitz, J.; Blum, R.; Dietrich, A.; Freichel, M.; Flockerzi, V.; Birnbaumer, L.; Konnerth, A. TRPC3 Channels Are Required for Synaptic Transmission and Motor Coordination. *Neuron* **2008**, *59*, 392−398.
(17) Lavender, V.; Chong, S.; Ralphs, K.; Wolstenholme, A. J.; Reaves, B. J. Increasing the expression of calcium-permeable TRPC3 and TRPC7 channels enhances constitutive secretion. *Biochem. J.* **2008**, *413*, 437−446.
(18) Alkhani, H.; Ase, A. R.; Grant, R.; O'Donnell, D.; Groschner, K.; Séguéla, P. Contribution of TRPC3 to Store-Operated Calcium Entry and Inflammatory Transductions in Primary Nociceptors. *Mol. Pain* **2014**, *10*, 43.
(19) Kang, F.; Zhou, M.; Huang, X.; Fan, J.; Wei, L.; Boulanger, J.; Liu, Z.; Salamero, J.; Liu, Y.; Chen, L. E-syt1 Re-arranges STIM1 Clusters to Stabilize Ring-shaped ER-PM Contact Sites and Accelerate Ca^{2+} Store Replenishment. *Sci. Rep.* **2019**, *9*, 3975.
(20) Liu, H.; Lin, W. Y.; Leibow, S. R.; Morateck, A. J.; Ahuja, M.; Muallem, S. TRPC3 channel gating by lipids requires localization at the ER/PM junctions defined by STIM1. *J. Cell Biol.* **2022**, *221*, No. e202107120.
(21) Zhou, F.-W.; Matta, S. G.; Zhou, F.-M. Constitutively Active TRPC3 Channels Regulate Basal Ganglia Output Neurons. *J. Neurosci.* **2008**, *28*, 473−482.
(22) Wan, L.; Molloy, S. S.; Thomas, L.; Liu, G.; Xiang, Y.; Rybak, S. L.; Thomas, G. PACS-1 Defines a Novel Gene Family of Cytosolic Sorting Proteins Required for trans-Golgi Network Localization. *Cell* **1998**, *94*, 205−216.
(23) Crump, C. M. PACS-1 binding to adaptors is required for acidic cluster motif-mediated protein traffic. *EMBO J.* **2001**, *20*, 2191−2201.
(24) Köttgen, M.; Benzing, T.; Simmen, T.; Tauber, R.; Buchholz, B.; Feliciangeli, S.; Huber, T. B.; Schermer, B.; Kramer-Zucker, A.; Höpker, K.; Simmen, K. C.; Tschucke, C. C.; Sandford, R.; Kim, E.; Thomas, G.; Walz, G. Trafficking of TRPP2 by PACS proteins represents a novel mechanism of ion channel regulation. *EMBO J.* **2005**, *24*, 705−716.
(25) Itagaki, K.; Kannan, K. B.; Singh, B. B.; Hauser, C. J. Cytoskeletal Reorganization Internalizes Multiple Transient Receptor Potential Channels and Blocks Calcium Entry into Human Neutrophils. *J. Immunol.* **2004**, *172*, 601−607.
(26) Ricotta, D.; Hansen, J.; Preiss, C.; Teichert, D.; Höning, S. Characterization of a Protein Phosphatase 2A Holoenzyme That Dephosphorylates the Clathrin Adaptors AP-1 and AP-2. *J. Biol. Chem.* **2008**, *283*, 5510−5517.
(27) Schuurs-Hoeijmakers, J. H. M.; Oh, E. C.; Vissers, L. E. L. M.; Swinkels, M. E. M.; Gilissen, C.; Willemsen, M. A.; Holvoet, M.; Steehouwer, M.; Veltman, J. A.; de Vries, B. B. A.; van Bokhoven, H.; de Brouwer, A. P. M.; Katsanis, N.; Devriendt, K.; Brunner, H. G. Recurrent De Novo Mutations in PACS1 Cause Defective Cranial-Neural-Crest Migration and Define a Recognizable Intellectual-Disability Syndrome. *Am. J. Hum. Genet.* **2012**, *91*, 1122−1127.
(28) Giordano, F.; Saheki, Y.; Idevall-Hagren, O.; Colombo, S. F.; Pirruccello, M.; Milosevic, I.; Gracheva, E. O.; Bagriantsev, S. N.; Borgese, N.; De Camilli, P. PI(4,5)P2-Dependent and Ca2+-Regulated ER-PM interactions mediated by the extended synaptotagmins. *Cell* **2013**, *153*, 1494−1509.
(29) Blom, N.; Sicheritz-Pontén, T.; Gupta, R.; Gammeltoft, S.; Brunak, S. Prediction of post-translational glycosylation and phosphorylation of proteins from the amino acid sequence. *Proteomics* **2004**, *4*, 1633−1649.
(30) Schermer, B.; Höpker, K.; Omran, H.; Ghenoiu, C.; Fliegauf, M.; Fekete, A.; Horvath, J.; Köttgen, M.; Hackl, M.; Zschiedrich, S.; Huber, T. B.; Kramer-Zucker, A.; Zentgraf, H.; Blaukat, A.; Walz, G.; Benzing, T. Phosphorylation by casein kinase 2 induces PACS-1 binding of nephrocystin and targeting to cilia. *EMBO J.* **2005**, *24*, 4415−4424.
(31) Blom, N.; Gammeltoft, S.; Brunak, S. Sequence and structure-based prediction of eukaryotic protein phosphorylation sites1 1Edited by F. E. Cohen. *J. Mol. Biol.* **1999**, *294*, 1351−1362.
(32) Kerppola, T. K. Bimolecular Fluorescence Complementation (BiFC) Analysis as a Probe of Protein Interactions in Living Cells. *Annu. Rev. Biophys.* **2008**, *37*, 465−487.
(33) Dirk, B. S.; Pawlak, E. N.; Johnson, A. L.; Van Nynatten, L. R.; Jacob, R. A.; Heit, B.; Dikeakos, J. D. HIV-1 Nef sequesters MHC-I intracellularly by targeting early stages of endocytosis and recycling. *Sci. Rep.* **2016**, *6*, 37021.
(34) Trothen, S. M.; Zang, R. X.; Lurie, A.; Dikeakos, J. D. PACS-1 contains distinct motifs for nuclear-cytoplasmic transport and interacts with the RNA-binding protein PTBP1 in the nucleus and cytosol. *FEBS Lett.* **2022**, *596*, 232−248.
(35) Tremblay, M. G.; Herdman, C.; Guillou, F.; Mishra, P. K.; Baril, J.; Bellenfant, S.; Moss, T. Extended Synaptotagmin Interaction with the Fibroblast Growth Factor Receptor Depends on Receptor Conformation, Not Catalytic Activity. *J. Biol. Chem.* **2015**, *290*, 16142−16156.
(36) Jackson, T. R.; Patterson, S. I.; Thastrup, O.; Hanley, M. R. A novel tumour promoter, thapsigargin, transiently increases cytoplasmic free Ca^{2+} without generation of inositol phosphates in NG115−401L neuronal cells. *Biochem. J.* **1988**, *253*, 81−86.
(37) Dirk, B. S.; End, C.; Pawlak, E. N.; Van Nynatten, L. R.; Jacob, R. A.; Heit, B.; Dikeakos, J. D. PACS-1 and adaptor protein-1 mediate ACTH trafficking to the regulated secretory pathway. *Biochem. Biophys. Res. Commun.* **2018**, *507*, 519−525.
(38) Xie, B.; Nguyen, P. M.; Idevall-Hagren, O. Feedback regulation of insulin secretion by extended synaptotagmin-1. *FASEB J.* **2019**, *33*, 4716−4728.
(39) Youker, R. T.; Shinde, U.; Day, R.; Thomas, G. At the crossroads of homoeostasis and disease: roles of the PACS proteins in membrane traffic and apoptosis. *Biochem. J.* **2009**, *421*, 1−15.
(40) Thomas, G.; Aslan, J. E.; Thomas, L.; Shinde, P.; Shinde, U.; Simmen, T. Caught in the act − protein adaptation and the expanding roles of the PACS proteins in tissue homeostasis and disease. *J. Cell Sci.* **2017**, *130*, 1865.
(41) Wedel, B. J.; Vazquez, G.; McKay, R. R.; Bird, G. St. J.; Putney, J. W. A Calmodulin/Inositol 1,4,5-Trisphosphate (IP3) Receptor-binding Region Targets TRPC3 to the Plasma Membrane in a Calmodulin/IP3 Receptor-independent Process. *J. Biol. Chem.* **2003**, *278*, 25758−25765.
(42) Bian, X.; Saheki, Y.; De Camilli, P. Ca^{2+} releases E-Syt1 autoinhibition to couple ER-plasma membrane tethering with lipid transport. *EMBO J.* **2018**, *37*, 219−234.
(43) Farfariello, V.; Gordienko, D. V.; Mesilmany, L.; Touil, Y.; Germain, E.; Fliniaux, I.; Desruelles, E.; Gkika, D.; Roudbaraki, M.; Shapovalov, G.; Noyer, L.; Lebas, M.; Allart, L.; Zienthal-Gelus, N.; Iamshanova, O.; Bonardi, F.; Figeac, M.; Laine, W.; Kluza, J.; Marchetti, P.; Quesnel, B.; Metzger, D.; Bernard, D.; Parys, J. B.; Lemonnier, L.; Prevarskaya, N. TRPC3 shapes the ER-mitochondria Ca2+ transfer characterizing tumour-promoting senescence. *Nat. Commun.* **2022**, *13*, 956.
(44) Nair-Gill, E.; Bonora, M.; Zhong, X.; Liu, A.; Miranda, A.; Stewart, N.; Ludwig, S.; Russell, J.; Gallagher, T.; Pinton, P.; Beutler, B. Calcium flux control by Pacs1-Wdr37 promotes lymphocyte quiescence and lymphoproliferative diseases. *EMBO J.* **2021**, *40*, No. e104888.
(45) Simmen, T.; Aslan, J. E.; Blagoveshchenskaya, A. D.; Thomas, L.; Wan, L.; Xiang, Y.; Feliciangeli, S. F.; Hung, C.-H.; Crump, C. M.; Thomas, G. PACS-2 controls endoplasmic reticulum−mitochondria communication and Bid-mediated apoptosis. *EMBO J.* **2005**, *24*, 717−729.
(46) Feng, S.; Li, H.; Tai, Y.; Huang, J.; Su, Y.; Abramowitz, J.; Zhu, M. X.; Birnbaumer, L.; Wang, Y. Canonical transient receptor potential 3 channels regulate mitochondrial calcium uptake. *Proc. Natl. Acad. Sci. U.S.A.* **2013**, *110*, 11011−11016.

https://doi.org/10.1021/acsomega.4c04998
ACS Omega 2024, 9, 35014−35027

(47) Brasacchio, D.; Alsop, A. E.; Noori, T.; Lufti, M.; Iyer, S.; Simpson, K. J.; Bird, P. I.; Kluck, R. M.; Johnstone, R. W.; Trapani, J. A. Epigenetic control of mitochondrial cell death through PACS1-mediated regulation of BAX/BAK oligomerization. *Cell Death Differ.* **2017**, *24*, 961−970.
(48) Pinton, P.; Giorgi, C.; Siviero, R.; Zecchini, E.; Rizzuto, R. Calcium and apoptosis: ER-mitochondria Ca2+ transfer in the control of apoptosis. *Oncogene* **2008**, *27*, 6407−6418.
(49) Thi My Nhung, T.; Phuoc Long, N.; Diem Nghi, T.; Suh, Y.; Hoang Anh, N.; Jung, C. W.; Minh Triet, H.; Jung, M.; Woo, Y.; Yoo, J.; Noh, S.; Kim, S. J.; Lee, S. B.; Park, S.; Thomas, G.; Simmen, T.; Mun, J.; Rhee, H.-W.; Kwon, S. W.; Park, S. K. Genome-wide kinase-MAM interactome screening reveals the role of CK2A1 in MAM Ca^{2+} dynamics linked to DEE66. *Proc. Natl. Acad. Sci. U.S.A.* **2023**, *120*, No. e2303402120.
(50) Rached, G.; Saliba, Y.; Maddah, D.; Hajal, J.; Smayra, V.; Bakhos, J.; Groschner, K.; Birnbaumer, L.; Fares, N. TRPC3 Regulates Islet Beta-Cell Insulin Secretion. *Adv. Sci.* **2023**, *10*, 2204846.
(51) Mani, C.; Tripathi, K.; Luan, S.; Clark, D. W.; Andrews, J. F.; Vindigni, A.; Thomas, G.; Palle, K. The multifunctional protein PACS-1 is required for HDAC2-and HDAC3-dependent chromatin maturation and genomic stability. *Oncogene.* **2020**, *39*, 2583−2596.
(52) Edie, S.; Zaghloul, N. A.; Leitch, C. C.; Klinedinst, D. K.; Lebron, J.; Thole, J. F.; McCallion, A. S.; Katsanis, N.; Reeves, R. H. Survey of Human Chromosome 21 Gene Expression Effects on Early Development in Danio rerio. *G3 (Bethesda)* **2018**, *8*, 2215−2223.
(53) Shukla, A. K.; Kim, J.; Ahn, S.; Xiao, K.; Shenoy, S. K.; Liedtke, W.; Lefkowitz, R. J. Arresting a transient receptor potential (TRP) channel: beta-arrestin 1 mediates ubiquitination and functional down-regulation of TRPV4. *J. Biol. Chem.* **2010**, *285*, 30115−30125.
(54) Prévost, J.; Edgar, C. R.; Richard, J.; Trothen, S. M.; Jacob, R. A.; Mumby, M. J.; Pickering, S.; Dubé, M.; Kaufmann, D. E.; Kirchhoff, F.; Neil, S.; Finzi, A.; Dikeakos, J. D. HIV-1 Vpu Downregulates Tim-3 from the Surface of Infected CD4+ T Cells. *J. Virol.* **2020**, *94*, e01999-19.
(55) Schindelin, J.; Arganda-Carreras, I.; Frise, E.; Kaynig, V.; Longair, M.; Pietzsch, T.; Preibisch, S.; Rueden, C.; Saalfeld, S.; Schmid, B.; Tinevez, J.-Y.; White, D. J.; Hartenstein, V.; Eliceiri, K.; Tomancak, P.; Cardona, A. Fiji: an open-source platform for biological-image analysis. *Nat. Methods* **2012**, *9*, 676−682.
(56) Balint, B.; Yin, H.; Chakrabarti, S.; Chu, M. W. A.; Sims, S. M.; Pickering, J. G. Collectivization of Vascular Smooth Muscle Cells via TGF-β−Cadherin-11−Dependent Adhesive Switching. *ATVB* **2015**, *35*, 1254−1264.
(57) Royston, P. Approximating the Shapiro-Wilk W-test for non-normality. *Stat. Comput.* **1992**, *2*, 117−119.

https://doi.org/10.1021/acsomega.4c04998
ACS Omega 2024, 9, 35014−35027